Analytica Chimica Acta 1158 (2021) 338413

Contents lists available at ScienceDirect

Analytica Chimica Acta

journal homepage: www.elsevier.com/locate/aca

Novel electrochemical biosensor based on Exo III-assisted digestion of dsDNA polymer from hybridization chain reaction in homogeneous solution for CYFRA 21-1 DNA assay

Changrui Feng [a], Chi Zhang [b], Jiaxin Guo [a], Gaiping Li [a], Baoxian Ye [a], Lina Zou [a, *]

[a] College of Chemistry, Green Catalysis Center, Zhengzhou University, Zhengzhou, 450001, PR China
[b] Department of Orthopedics, First Affiliated Hospital of Zhengzhou University, Zhengzhou, 450001, PR China

HIGHLIGHTS

- A novel strategy based on Exo III-assisted digestion of dsDNA polymer (EADDP) was proposed.
- The Exo III was firstly used to digest dsDNA polymer to produce abundant double signal fragments (DSF).
- The EADDP can convert one target into large amount of DSF in homogeneous solution.
- EADDP in homogeneous solution and direct capture of DSF simplified the operation steps on electrode.
- This biosensor achieved a low detection limit of 0.0348 fM for CYFRA 21-1 DNA detection.

GRAPHICAL ABSTRACT

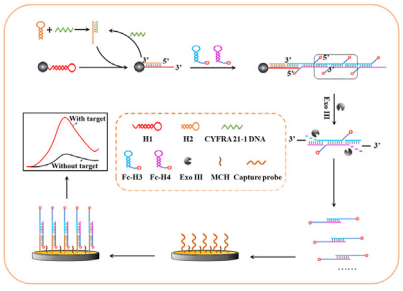

ARTICLE INFO

Article history:
Received 16 January 2021
Received in revised form
1 March 2021
Accepted 11 March 2021
Available online 16 March 2021

Keywords:
Catalytic hairpin assembly
Hybridization chain reaction
Exonuclease III
Homogeneous solution
Double signal fragments

ABSTRACT

A novel electrochemical biosensing strategy was proposed to detect cytokeratin fragment antigen 21-1 (CYFRA 21-1) DNA based on Exo III-assisted digestion of dsDNA polymer (EADDP) from hybridization chain reaction (HCR). Primarily, the presence of target can drive a catalytic hairpin assembly (CHA) reaction, which was aimed to achieve target recognition and circulation. Then the HCR can be triggered for further signal amplification and generate long dsDNA polymer with signal tags. Subsequently, the introduction of Exo III can digest the long dsDNA polymer to produce large amounts of double signal fragments (DSFs). The above experiments were all carried out in homogeneous solution. Finally, the released DSF can be captured onto the electrode directly by capture probe (CP) and a highly amplified electrochemical signal can be detected. The EADDP in homogeneous solution circumvented complex solid-liquid interface reaction and tedious operation steps on electrode. Besides, one target can be converted into abundant DSFs, which greatly improved the sensitivity. This biosensor exhibited a low detection limit (0.0348 fM) and wide linear range (5 fM ~ 50 nM) for CYFRA 21-1 DNA biosensing with reliable specificity and stability.

1. Introduction

Lung cancer is a kind of malignant tumors that threats people's

* Corresponding author.
E-mail address: zoulina@zzu.edu.cn (L. Zou).

https://doi.org/10.1016/j.aca.2021.338413
0003-2670/

health and life greatly. It is roughly fall into small cell lung cancer (SCLC) and non-small cell lung cancer (NSCLC) and NSCLC accounts for higher proportion (~80%) [1–4]. Cytokeratin fragment antigen 21-1 (CYFRA 21-1) DNA is considered as a tumor biomarker mainly used to detect lung cancer, especially for the diagnosis of NSCLC [5,6]. The serum level of it ought to be 0–1 cps/μL and is positively correlated with the clinical stage of tumor and can also be used as an effective indicator to track early recurrence after lung cancer surgery and chemoradiotherapy [7,8]. As a result, it is of great significance to detect CYFRA 21-1 DNA in genetic level for more effectively early diagnosis and prognosis of lung cancer.

So far, many approaches have been explored for sensitive detection of cancer biomarkers. For instance, fluorescence [9,10], surface plasmon resonance [11,12], enzyme-linked immunosorbent assay (ELISA) [13,14] and electrochemistry [15,16]. Among them, electrochemistry shows great advantage due to its low cost, easy operation, rapid response and high sensitivity. However, in the early stage of lung cancer, CYFRA 21-1 DNA expresses at low level, which severely limits the early diagnosis of cancer. Therefore, it is very necessary to propose an effective electrochemical strategy for ultrasensitive CYFRA 21-1 DNA detection.

In order to achieve high sensitivity, a lot of amplification methods have been put forward. Hybridization chain reaction (HCR) is an isothermal amplification strategy with no need of enzyme [17,18]. Its high amplification efficiency makes it widely used in constructing electrochemical biosensors. Normally, the HCR occurs on the electrode surface to form long dsDNA structure and carry more electrochemical tags [19–21]. Due to the limitation of electrode surface area, the reaction efficiency is often restricted by steric hindrance [22]. Moreover, for the complexity of solid-liquid interface reaction, it usually takes a long time to get the optimal signal. So, in order to improve the reaction efficiency and reduce electrode operation steps, some works reported HCR occurred in homogeneous solution [22–24]. Nonetheless, because of the large size of the formed long dsDNA, it is difficult to be transferred from homogeneous solution to the electrode surface. Exonuclease III is a common DNA treating tool that often used to degrade dsDNA from blunt ends, 3' - concave ends or nicks [25–27]. Based on this property, it can be used to convert the long dsDNA into short strands to allow them to be captured onto the electrode surface more easily.

Inspired by these, the Exo III was firstly used to digest the long dsDNA formed by HCR in homogeneous solution to fabricate a novel electrochemical biosensor. Here, a catalytic hairpin assembly (CHA) process was firstly designed for target recognition and circulation. Then the HCR was employed for further amplification. As a result, long dsDNA polymer with signal tags were formed. Then Exo III-assisted digestion of dsDNA polymer (EADDP) was utilized to convert one target into large amounts of DSFs, which can be captured onto the electrode by capture probe (CP) and generated electrochemical signal directly. By using this strategy, the amplification effect of HCR can be realized and the steric hindrance can be effectively circumvented at the same time. In addition, the electrode operation process was greatly simplified due to the EADDP in solution and direct capture of DSFs. Taking above advantages, this biosensor can detect CYFRA 21-1 DNA at a very low level and possessed satisfactory specificity and stability.

2. Experimental section

2.1. Connection of H1 to carboxylated magnetic beads

The hairpin probe H1 was immobilized on carboxylated magnetic beads (MBs, 5 mg/mL, 500–600 nm) through amido bond [28,29]. In brief, 100 μL of MBs were washed with PBS buffer three times (0.1 M, pH 7.4). Then EDC (20 mg/mL) and NHS (40 mg/mL) were used to activate carboxyl groups on MBs. After that, 500 μL of H1 (1 μM) were mixed with MBs solution and put them into a thermostatic oscillator to incubate at 37 °C overnight. After the reaction, the H1-MBs complex were separated magnetically and washed repeatedly. Then they were re-dispersed in PBS buffer (200 μL, 0.1 M, pH 7.4).

2.2. EADDP process in homogeneous solution

Target DNA and 1 μM hairpin probe H2 (10 μL each) were firstly incubated with 5 μL of H1-MBs for 2 h at 37 °C with gentle shaking to unfold H1. Then 100 μL of mixed solution including ferrocene modified H3 and H4 (0.5 μM) were added to participate the hybridization chain reaction (HCR) for 1.5 h at 37 °C. Afterwards, 50 μL of solution containing 5 μL of 20 $U \cdot \mu L^{-1}$ Exo III and 10 mM tris-HCl buffer (10 mM, pH 7.4) were reacted with the separated magnetic beads for 2 h with gentle shaking to digest the duplex structure formed by HCR. After magnetic separation, supernatant containing large amounts of DSFs can be obtained.

2.3. Electrochemical measurements

The pretreatment and gold nanoparticles deposition of GCE were the same as previous work [30]. Subsequently, the thiol-modified capture probes (CP, 1 μM) which was annealed with TCEP (100 mM) to cut the S–S bond before were incubated on electrode at 25 °C overnight. After that, the electrode was blocked with 6-mercapto-1-hexanol (MCH, 1 mM) for 40 min. Then 10 μL of magnetic separated supernatant obtained above were dropped onto the electrode to react for 2 h at 37 °C. Afterwards, the signal was measured by DPV through immersed the electrode into PBS buffer (2 mL, 10 mM, pH 7.4).

2.4. Polyacrylamide gel electrophoresis

Firstly, ultrapure water, 5 × TBE, acrylamide (30%), TEMED and APS (10%) were added in appropriate proportion and mixed thoroughly to prepare a 12% polyacrylamide gel. Then the prepared gel was washed with water and 1 × TBE three times each. After that, micro-syringe was used to inject the preprepared samples (1 μM each) into the gel. Then set the voltage of electrophoresis apparatus to 80 V and the time to 90 min to run this experiment in 1 × TBE buffer. After finished the process, a UV light was used to visual the gel image.

2.5. Base mismatched experiment

Non complementary DNA (NC), three-base mismatched DNA (TM) and single-base mismatched DNA (SM) with same volume (10 μL) and concentration (1 nM) were chosen to replace target DNA and proceed a series of reactions as described in section 2.2 and 2.3 under identical experimental conditions. Afterwards, the electrochemical signals of them were measured by DPV through immersed the electrode into PBS buffer (2 mL, 10 mM, pH 7.4).

3. Results and discussion

3.1. Design principle of proposed biosensor

As shown in Scheme 1, the biosensing process was mainly composed of two parts. (A) Catalytic hairpin assembly (CHA) assisted target recycling and Exo III assisted digestion of dsDNA polymer (EADDP) from hybridization chain reaction in homogeneous solution. (B) One-step capture of double signal fragments

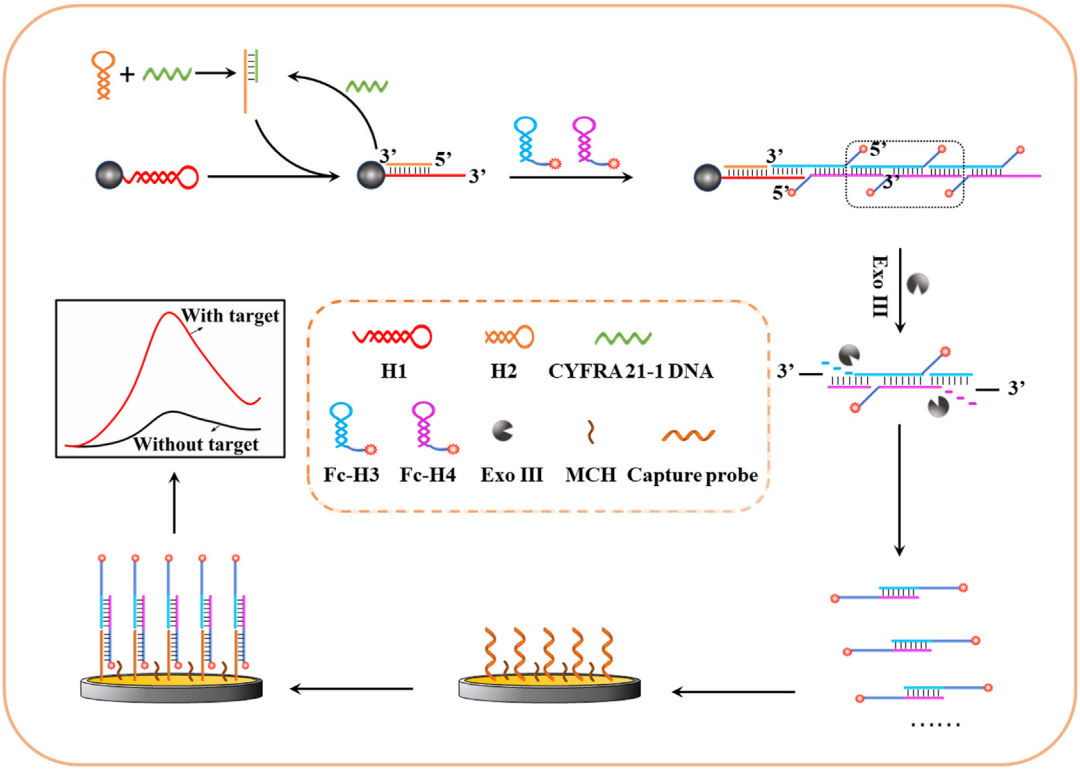

Scheme 1. Schematic illustration of proposed biosensor based on EADDP in homogeneous solution for detection of CYFRA 21-1 DNA.

(DSF) on electrode. Firstly, the hairpin probe H1 was immobilized on the magnetic beads (MBs) via amido bond to form H1-MBs. Then the mixture of target and H2 were added to activate catalytic hairpin assembly (CHA) reaction for the purpose of opening H1 as well as target recycling. After that, the H3 and H4, which had the same extended sequence at 5′-terminal with ferrocene modification were introduced into the reaction system. The unfolded sequence of H1 can act as trigger to initiate HCR in the presence of them. Subsequently, long dsDNA polymer with ferrocene modification was formed. Then Exo III was utilized to digest the long dsDNA from 3′ to 5′ terminal. After magnetic separation, large amount of DSFs produced in the supernatant. After the pretreatment and modification of electrode, the DSF can be captured onto the electrode by capture probe (CP) in one step and generated electrochemical signal at the same time. As a result, by combing CHA assisted target recycling, HCR amplification, and EADDP, this biosensor achieved ultrasensitive detection of CYFRA 21-1 DNA.

3.2. Electrochemical characterization of electrode modification

The immobilization process of electrode was firstly characterized by cyclic voltammetry (CV) through using $[Fe(CN)_6]^{3-/4-}$ (5 mM, 0.1 M KCl) as redox probe. As shown in Fig. 1A, The CV curve of bare GCE was a couple of well-defined redox peaks (curve a). Then the peak current was increased after electrodeposition of gold nanoparticles due to their excellent electron conductivity (curve b). After the modification of CP, because of the repulsive interaction between $[Fe(CN)_6]^{3-/4-}$ probe and electronegative phosphate backbone of DNA, the peak current dropped obviously (curve c). After treated with MCH, slightly decrease of peak current can be seen probably because of its electron transfer blocking (curve d). Subsequently, the incubation with DSF made the peak current further reduced due to its further enhancement of repulsive interaction (curve e).

The charge transfer process of different modified electrode interfaces can be investigated by electrochemical impedance spectroscopy (EIS). The semicircle diameter of the EIS curve is a very important parameter, which equals to charge transfer resistance (R_{ct}). Therefore, the fabrication process can be also characterized by EIS. As demonstrated in Fig. 1B, the impedance of bare GCE was very small which equals to 14.85 Ω (curve a), and it got smaller after deposited with gold nanoparticles ($R_{ct} = 6.148$ Ω) due to its electron transfer facilitation (curve b). After incubated with CP, the R_{ct} value increased dramatically to 1301 Ω (curve c) owing to the electrostatic repulsion between charge negative redox probe and phosphate skeleton of DNA. The impedance was increased further after blocking with non-conductive MCH (curve d, $R_{ct} = 1700$ Ω). Finally, a significant increase of resistance can be seen after incubation with DSF (curve e, $R_{ct} = 2973$ Ω) for DSFs enhanced the negative charge on the electrode surface. The results indicated by these trends were in good agreement with CV. Taking above results shown that the biosensor was assembled as expected.

3.3. Experimental proof of the proposed assay

In order to explore the feasibility of proposed strategy, polyacrylamide gel electrophoresis (PAGE) and differential pulse voltammetry (DPV) were used to record the experimental phenomenon under different conditions. Firstly, PAGE was used to verify the CHA and HCR processes. As shown in Fig. 2A, lane 5 represented the mixture of target (lane 2, the band of it was missed because of its small molecular weight) and H2 (lane 4) and it run slower than either of them. This indicated that the target can unfold H2 successfully. Lane 6 exhibited the CHA process and an obvious new band appeared which represented the complex of H1 and H2. This demonstrated that the CHA can succeed in the presence of

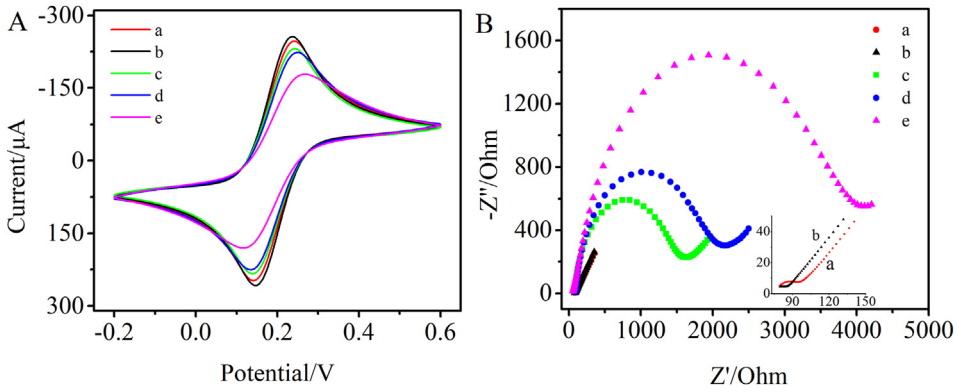

Fig. 1. (A) CV and (B) EIS characterization of stepwise modification on electrode. (a) bare GCE, (b) depAu/GCE, (c) CP/depAu/GCE, (d) MCH/CP/depAu/GCE, (e) DSF/MCH/CP/depAu/GCE. (Frequency range of EIS: 0.1 Hz-10 kHz. Inset in EIS: An enlarged superposition of curves a and b).

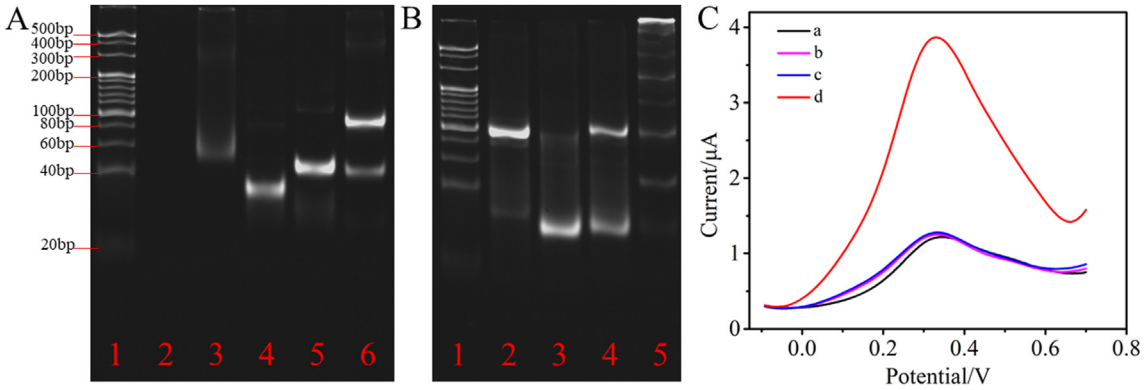

Fig. 2. (A) PAGE for CHA characterization, lane 1: Marker, lane 2: Target, lane 3: H1, lane 4: H2, lane 5: Target + H2, lane 6: CHA process, (B) PAGE for HCR characterization, lane 2: H3, lane 3: H4, lane 4: HCR process in the absence of target, lane 5: HCR process in the presence of target. (C) DPV results under different conditions; curve a: In the absence of target, curve b: In the absence of HCR process; curve c: In the absence of Exo III; curve d: In the presence of target, HCR and Exo III.

target. In Fig. 2B, lane 4 expressed the HCR process without target, while lane 5 was the opposite. By comparison of their bands, it can be clearly seen that only when target existed (lane 5), a series of bands with different molecular weights (MW) and a very bright band with large MW appeared. This declared that the HCR can only take place with the existence of target.

As shown in Fig. 2C, curve a represented the DPV signal response in the absence of target, only negligible peak current can be observed. When the HCR did not proceed (curve b) or there were no Exo III (curve c), the current responses were almost the same as without target, this was because that the DSF did not generate in the final supernatant without either of them. However, when the target, HCR and Exo III coexisted, strong and obvious peak current can be seen for large amounts of DSFs generated and were captured onto the electrode. All the results suggested that the proposed biosensor based on EADDP from HCR in homogeneous solution for CYFRA 21-1 detection was reliable.

3.4. Optimization of experimental parameters

In order to obtain the optimal analytical performance of constructed biosensor for detecting target DNA, some important experimental conditions were optimized by DPV. Firstly, the reaction time of CHA was investigated owing to its impact on the number of unfolded H1. This had implications for the following HCR process. When optimized this condition, the reaction time of HCR and Exo III were all settled as 120 min and the concentration of Exo III was 2 U μL^{-1}. As shown in Fig. 3A, the current increased at first as time growing from 30 min to 120 min and reached a plateau after 120 min, so the reaction time of CHA was settled as 120 min.

The time of HCR would influence the amount of signal labels carried in the formed long dsDNA structure and then had effect on the quantity of DSF. So it was necessary to explore this experimental condition. Besides, the reaction time of CHA was 120 min, the concentration and digestion time of Exo III were 2 U μL^{-1} and 120 min respectively under this condition optimization. As demonstrated in Fig. 3B, the current increased with increasing time and nearly remained stable after 90 min. As a result, the optimal reaction time for HCR was determined as 90 min.

The concentration and digestion time of Exo III all had an impact on the amount of DSF and then affected the electrochemical signal. Under the concentration optimization of Exo III, the reaction time of CHA, HCR and Exo III were 120 min, 90 min and 120min respectively. While for the digestion time of Exo III, other parameters were as follows, the reaction time of CHA and HCR were 120 min and 90 min, the concentration of Exo III was 2 U μL^{-1}. As illustrated in Fig. 3C, the current responses increased as concentration goes from 0.5 U μL^{-1} to 2 U μL^{-1} and remained unchanged basically after 2 U μL^{-1}. Therefore, the optimal concentration of Exo III was confirmed as 2 U μL^{-1}. As shown in Fig. 3D, the signal results increased as digestion time increasing from 30 min to 120 min and obtained saturated signal after 120 min, so the digestion time of Exo III was optimized as 120 min.

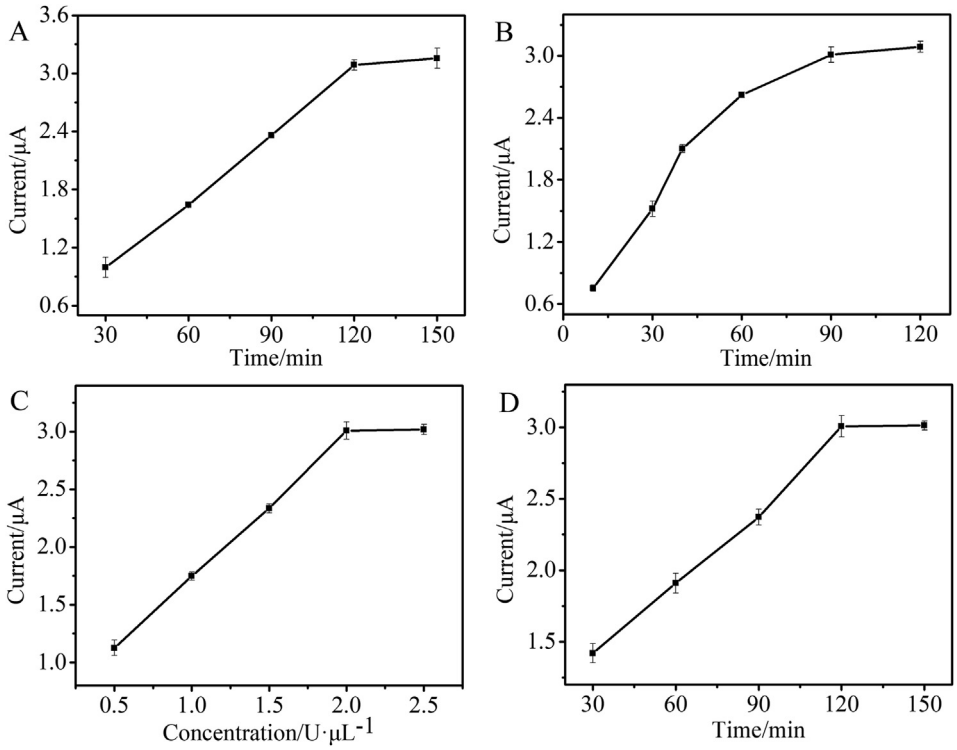

Fig. 3. Optimization of experimental conditions. (A) Reaction time of CHA, (B) Reaction time of HCR process. (C) Concentration of Exo III. (D) Digestion time of Exo III. (Target concentration: 1 nM).

3.5. Electrochemical assay for target DNA detection

To evaluate the electrochemical detection performance of this biosensor, under optimal experimental conditions, the signal results were recorded under different concentrations of CYFRA 21-1 DNA. In Fig. 4A, the current intensity gradually increased with the increasing concentration of CYFRA 21-1. The linear fitting curve was demonstrated in Fig. 4B, it can be clearly seen that in the concentration range from 5 fM to 50 nM, there was a good linear relationship between the peak current and the logarithm of target concentration. The linear fitting equation is $I = 0.3505\ \mathrm{lgC} + 1.8928$ ($R^2 = 0.9933$) and the limit of detection for CYFRA 21-1 DNA was calculated to be 0.0348 fM (S/N = 3). Compared with other reported biosensors for cancer biomarker detection (Table S2), this novel biosensor is not inferior in analytical performance.

3.6. Specificity, repeatability and stability investigation

To evaluate the specificity of fabricated biosensor, the electrochemical signals generated from same amount of interferents with different mismatched bases were recorded to compare with target DNA (T) and blank (B). As shown in Fig. 5A, the current of non-complementary target DNA (NC) was almost identical to blank, and there was only a slight difference in the current of three-base mismatched target DNA (TM) and blank. With regards to single-base mismatched target DNA (SM), its electrochemical signal was approximately 19.42% of target DNA after deducting the blank. This demonstrated favorable specificity of the biosensor and it can

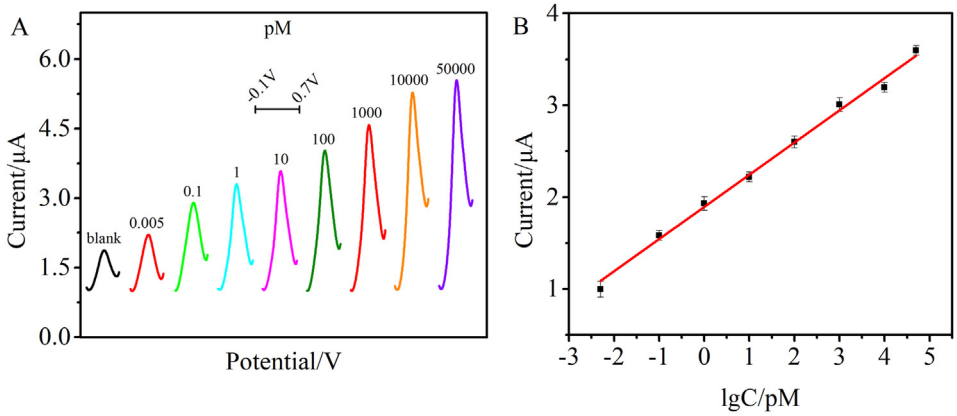

Fig. 4. (A) The DPV results of constructed biosensor under different concentrations of CYFRA 21-1 DNA. (B) The linear relationship between the DPV peak current and the logarithm value of CYFRA 21-1 DNA concentration. (Error bars, SD; n = 3).

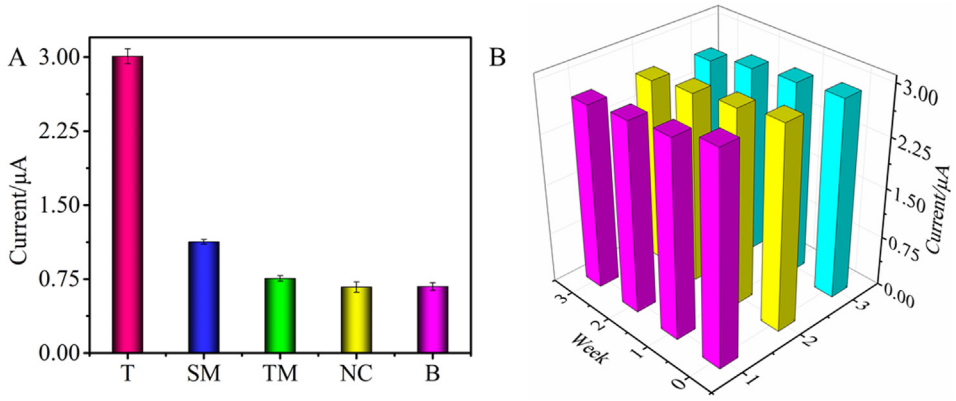

Fig. 5. (A) The current results toward 1 nM different DNA sequences. From left to right are target DNA (T), single-base mismatched DNA (SM), three-base mismatched DNA (TM), non-complementary DNA (NC) and blank (B). (B) The stability of this biosensor for detecting target DNA (1 nM).

Table 1
Real sample analysis of proposed biosensor for CYFRA 21-1 DNA spiked in diluted human serum.

Samples	Added CYFRA 21-1 (pM)	Found CYFRA 21-1 (pM)	Relative standard deviation (%)	Recovery (%)
1	0.01	0.0107	4.65	106.80
2	1	1.0354	3.09	103.54
3	10	10.4232	1.55	104.23
4	1000	981.0700	1.34	98.11
5	5000	4864.0720	1.46	97.28

effectively discriminate single-base mismatched DNA.

The repeatability of this biosensor was investigated through a set of parallel experiment. Six independent electrodes were used and their electrochemical signals were determined under identical experimental conditions. The relative standard derivation (RSD) was calculated as 2.16%, which declared that this biosensor possessed recommendable repeatability.

The stability of constructed biosensor was also explored by storing it at 4 °C in the refrigerator and measured the electrochemical signal every one week (Fig. 5B). The current was about 96.12% and 93.45% as it was in the beginning after one and two weeks respectively. Even after three weeks, the signal response was still kept at 89.95% of its initial value, which suggested satisfactory stability of this biosensor.

3.7. Real sample analysis

To assess the clinical application of constructed biosensor for detecting CYFRA 21-1 DNA, the recovery experiment was carried out by spiking five different concentrations of target DNA into 10-fold diluted healthy human serum samples. Table 1 listed the recovery rates and relative standard deviation (RSD) of the recovery experiment and the values are all within an acceptable range. The above results indicated that this biosensor might become a promising platform for clinical diagnosis of NSCLC.

4. Conclusion

This work proposed a novel strategy based on Exo III assisted digestion of dsDNA polymer (EADDP) from HCR in homogeneous solution to construct an electrochemical platform for target DNA biosensing. With the assistance of CHA, target recycling was achieved. After EADDP, large amount of DSF generated which can be captured onto the electrode surface directly to produce signal response. By using this strategy, the amplification ability of HCR was enhanced for one target input can output a tremendous number of DSFs. Besides, the steps on electrode can be greatly simplified for homogeneous reaction of EADDP. As a result, this biosensor achieved an ultralow detection limit of 0.0348 fM for CYFRA 21-1 DNA determination by integrating CHA and EADDP. Furthermore, it also possessed considerable potential in application of clinical diagnosis of NSCLC.

Declaration of competing interest

The authors declare that they have no known competing financial interests or personal relationships that could have appeared to influence the work reported in this paper.

Acknowledgements

The authors are sincerely grateful for the financial support from the National Natural Science Foundation of China (Grant no. U1504216; 21575130).

Appendix A. Supplementary data

Supplementary data to this article can be found online at https://doi.org/10.1016/j.aca.2021.338413.

Author Contribution

Changrui Feng, Conceptualization; Methodology; Validation; Resources; Data curation; Writing – original draft; Writing – review & editing; Chi Zhang, Formal analysis; Investigation; Jiaxin Guo, Validation; Formal analysis; Methodology; Investigation; Gaiping Li Formal analysis; Methodology; Investigation; Baoxian Ye, Formal analysis; Methodology; Investigation; Lina Zou, Data curation; Writing – review & editing; Project administration.

References

[1] S.K. Arya, S. Bhansali, Lung cancer and its early detection using biomarker-based biosensors, Chem. Rev. 111 (2011) 6783–6809.

[2] Q. Hu, D. Han, S. Gan, Y. Bao, L. Niu, Surface-initiated-reversible-addition-fragmentation-chain-transfer polymerization for electrochemical DNA biosensing, Anal. Chem. 90 (2018) 12207–12213.

[3] J.W. Hyun, S.H. Kim, S.H. Hwang, H.S. Gwak, H.J. Kim, The diagnostic and prognostic value of CSF cyfra 21-1 in patients with leptomeningeal metastasis of non-small cell lung cancer, J. Thorac. Oncol. 12 (2017) S958–S959.

[4] T. Muley, Y. He, V. Rolny, J. Riedlinger, B. Wehnl, F. Dayyani, et al., The combination of serum biomarkers CYFRA 21-1 and CEA in the prognostication of early stage non-small cell lung cancer (NSCLC), J. Thorac. Oncol. 10 (2015), S382-S382.

[5] L. Zhao, H. Yang, X. Zheng, J. Li, L. Jian, W. Feng, et al., Dual signal amplification by polysaccharide and eATRP for ultrasensitive detection of CYFRA 21-1 DNA, Biosens. Bioelectron. 150 (2020), 111895.

[6] X. Wang, Y. Zhang, L. Zhao, D. Wang, H. Yang, J. Kong, Polysaccharide-enhanced ARGET ATRP signal amplification for ultrasensitive fluorescent detection of lung cancer CYFRA 21-1 DNA, Anal. Bioanal. Chem. 412 (2020) 2413–2421.

[7] Y. Yu, Z. Huang, Y. Zhou, L. Zhang, A. Liu, W. Chen, et al., Facile and highly sensitive photoelectrochemical biosensing platform based on hierarchical architectured polydopamine/tungsten oxide nanocomposite film, Biosens. Bioelectron. 126 (2019) 1–6.

[8] J.W. Xue, L. Yang, Y. Du, Y. Ren, X. Ren, H.M. Ma, et al., Electrochemiluminescence sensing platform based on functionalized poly-(styrene-co-maleicanhydride) nanocrystals and iron doped hydroxyapatite for CYFRA 21-1 immunoassay, Sens. Actuator B. Chem 321 (2020) 8.

[9] W. Liu, L. Ma, Z. Guo, T. Liu, Y. Liu, J. Kong, et al., A Fluorescent sensor based on reversible addition-fragmentation chain transfer polymerization for the early diagnosis of non-small cell lung cancer, Anal. Sci. 36 (2020) 681–686.

[10] D.X. Wang, J. Wang, Y.X. Cui, Y.X. Wang, A.N. Tang, D.M. Kong, Nanolantern-based DNA probe and signal amplifier for tumor-related biomarker detection in living cells, Anal. Chem. 91 (2019) 13165–13173.

[11] X. Wang, T. Hou, H. Lin, W. Lv, H. Li, F. Li, In situ template generation of silver nanoparticles as amplification tags for ultrasensitive surface plasmon resonance biosensing of microRNA, Biosens. Bioelectron. 137 (2019) 82–87.

[12] C. Zhou, H. Zou, C. Sun, D. Ren, J. Chen, Y. Li, Signal amplification strategies for DNA-based surface plasmon resonance biosensors, Biosens. Bioelectron. 117 (2018) 678–689.

[13] Y.S. Yang, K. Smith-McCune, T.M. Darragh, Y. Lai, J.H. Lin, T.C. Chang, et al., Direct human papillomavirus E6 whole-cell enzyme-linked immunosorbent assay for objective measurement of E6 oncoproteins in cytology samples, Clin. Vaccine Immunol. 19 (2012) 1474–1479.

[14] L.F. Cheow, S.H. Ko, S.J. Kim, K.H. Kang, J. Han, Increasing the sensitivity of enzyme-linked immunosorbent assay using multiplexed electrokinetic concentrator, Anal. Chem. 82 (2010) 3383–3388.

[15] L. Xu, Z. Liu, S. Lei, D. Huang, L. Zou, B. Ye, A sandwich-type electrochemical aptasensor for the carcinoembryonic antigen via biocatalytic precipitation amplification and by using gold nanoparticle composites, Mikrochim. Acta 186 (2019) 473.

[16] M. Senel, M. Dervisevic, F. Kokkokoglu, Electrochemical DNA biosensors for label-free breast cancer gene marker detection, Anal. Bioanal. Chem. 411 (2019) 2925–2935.

[17] Z. Liu, S. Lei, L. Zou, G. Li, L. Xu, B. Ye, A label-free and double recognition-amplification novel strategy for sensitive and accurate carcinoembryonic antigen assay, Biosens. Bioelectron. 131 (2019) 113–118.

[18] Z. Chen, Y. Liu, C. Xin, J. Zhao, S. Liu, A cascade autocatalytic strand displacement amplification and hybridization chain reaction event for label-free and ultrasensitive electrochemical nucleic acid biosensing, Biosens. Bioelectron. 113 (2018) 1–8.

[19] H. Cheng, J. Liu, W. Ma, S. Duan, J. Huang, X. He, et al., Low background cascade signal amplification electrochemical sensing platform for tumor-related mRNA quantification by target-activated hybridization chain reaction and electroactive cargo release, Anal. Chem. 90 (2018) 12544–12552.

[20] X. Peng, J. Zhu, W. Wen, T. Bao, X. Zhang, H. He, et al., Silver nanoclusters-assisted triple-amplified biosensor for ultrasensitive methyltransferase activity detection based on AuNPs/ERGO hybrids and hybridization chain reaction, Biosens. Bioelectron. 118 (2018) 174–180.

[21] H. Zhang, Y. Yang, H. Dong, C. Cai, A superstructure-based electrochemical assay for signal-amplified detection of DNA methyltransferase activity, Biosens. Bioelectron. 86 (2016) 927–932.

[22] X. Huang, J. Jia, Y. Lin, B. Qiu, Z. Lin, H. Chen, A highly sensitive electrochemiluminescence biosensor for pyrophosphatase detection based on click chemistry-triggered hybridization chain reaction in homogeneous solution, ACS Appl. Mater. Interfaces 12 (2020) 34716–34722.

[23] L. Tian, J. Qi, O. Oderinde, C. Yao, W. Song, Y. Wang, Planar intercalated copper (II) complex molecule as small molecule enzyme mimic combined with Fe3O4 nanozyme for bienzyme synergistic catalysis applied to the microRNA biosensor, Biosens. Bioelectron. 110 (2018) 110–117.

[24] Z. Shen, L. He, W. Wang, L. Tan, N. Gan, Highly sensitive and simultaneous detection of microRNAs in serum using stir-bar assisted magnetic DNA nanospheres-encoded probes, Biosens. Bioelectron. 148 (2020), 111831.

[25] Z. Liu, S. Lei, L. Zou, G. Li, B. Ye, Grafting homogenous electrochemical biosensing strategy based on reverse proximity ligation and Exo III assisted target circulation for multiplexed communicable disease DNA assay, Biosens. Bioelectron. 167 (2020), 112487.

[26] X. Huang, W. Niu, J. Wu, Y. Wang, C. Li, J. Qiu, et al., A triple-amplification differential pulse voltammetry for sensitive detection of DNA based on exonuclease III, strand displacement reaction and terminal deoxynucleotidyl transferase, Biosens. Bioelectron. 143 (2019), 111609.

[27] X. Zheng, L. Li, L. Zhang, L. Xie, X. Song, J. Yu, Multiple self-cleaning paper-based electrochemical ratiometric biosensor based on the inner reference probe and exonuclease III-assisted signal amplification strategy, Biosens. Bioelectron. 147 (2020), 111769.

[28] T. Yu, P.P. Dai, J.J. Xu, H.Y. Chen, Highly sensitive colorimetric cancer cell detection based on dual signal amplification, ACS Appl. Mater. Interfaces 8 (2016) 4434–4441.

[29] H. Dong, H. Chen, J. Jiang, H. Zhang, C. Cai, Q. Shen, Highly sensitive electrochemical detection of tumor exosomes based on aptamer recognition-induced multi-DNA release and cyclic enzymatic amplification, Anal. Chem. 90 (2018) 4507–4513.

[30] X. Zhang, Z. Yang, Y. Chang, M. Qing, R. Yuan, Y. Chai, Novel 2D-DNA-nanoprobe-mediated enzyme-free-target-recycling amplification for the ultrasensitive electrochemical detection of microRNA, Anal. Chem. 90 (2018) 9538–9544.